

Nonlinear Photonics of Backward Waves

Alexander K. Popov¹ and Sergey A. Myslivets²

¹ Department of Physics & Astronomy, University of Wisconsin-Stevens Point,
Stevens Point, WI 54481-3897, USA, E-mail: apopov@uwsp.edu

² Institute of Physics, Siberian Division of the Russian Academy of Sciences,
660036 Krasnoyarsk, Russian Federation, E-mail: sam@iph.krasn.ru

Abstract

Several nonlinear-optical coupling schemes in double domain positive/negative index metamaterials are proposed, which include ordinary and backward electromagnetic waves. One of them is investigated in the context of the applications to compensating strong losses inherent to plasmonic metamaterials and to design of novel ultracompact photonic devices for optical sensing and data processing. Each of the schemes provides different distribution of the coupled fields (hot zones) across the originally strongly absorbing metamaterial slab and exotic output behavior compared with the counterparts in ordinary materials. The outlined possibilities are illustrated with the numerical simulations.

1 Introduction

Nanostructured negative-index metamaterials (NIMs) form a novel class of artificial electromagnetic materials that promises revolutionary breakthroughs in photonics. Such metamaterials are expected to play a key role in the development of novel photonic microdevices and all-optical data processing chips. Significant progress has been achieved recently in the design of bulk, multilayered, negative-index, plasmonic slabs. The problem, however, is that these structures introduce strong losses inherent to metals that are difficult to avoid. Unlike ordinary materials, the energy flow and wave vector (phase velocity) are counter-directed in NIMs. Negative-index properties and, therefore, backwardness of electromagnetic waves are usually achievable only within a certain wavelength band. Metamaterials remain ordinary, positive index, outside such interval. This opens the opportunities of unique schemes of nonlinear-optical coupling between the ordinary and backward electromagnetic waves, which meet the requirements of the phase matching. It is because all wave vectors remain parallel, whereas some of the energy flows inside the metamaterial appear counter-directed. Such unusual nonlinear propagation processes exhibit extraordinary properties not achievable in ordinary nonlinear optical materials and not described in the literature [1-6]. This paper is to propose several such coupling schemes and to present analysis of the operational properties for one of them in the context of their applications to compensating strong losses inherent to plasmonic metamaterials and to design novel photonic devices for to optical sensing and data processing. Each of the schemes provides different distribution of the coupled fields (hot zones) across the originally strongly absorbing metamaterial slab. The outlined possibilities to implement originally strongly absorbing microscopic samples of plasmonic metal-dielectric composites for the remote all-optically tailoring of their transparency and reflectivity as well as the options for creating of unique ultracompact photonic sensing devices is demonstrated through numerical simulations. Different schemes of coherent energy transfer from strong control field to the negative-index signals described here present alternative approaches to compensating losses in NIMs based on the population inversion (such as recent breakthrough reported in [7]).

2 Basic Idea and Coupling Schemes

2.0.1 Backward Waves

A striking electromagnetic property of negative-index (NI) metamaterials (NIMs) stems from the fact that energy flow and phase velocity of electromagnetic waves become counter-directed inside the NIM slab. Such phenomenon of backwardness of electromagnetic waves does not exist in naturally occurring materials. The appearance of *backward* electromagnetic waves (BW) can be explain as follows. The relations between the vectors of the electric and magnetic components and the wave-vector of the electromagnetic wave traveling in a transparent matter are given by:

$$\mathbf{k} \times \mathbf{E} = \frac{\omega}{c} \mu \mathbf{H}, \quad \mathbf{k} \times \mathbf{H} = -\frac{\omega}{c} \epsilon \mathbf{E}, \quad \sqrt{\epsilon} E = -\sqrt{\mu} H. \quad (1)$$

Equations (1) show that the vector triplet \mathbf{E} , \mathbf{H} , \mathbf{k} forms a right-handed system for an ordinary medium with $\epsilon > 0$ and $\mu > 0$. Simultaneously negative ϵ and μ result in a *left-handed* triplet and negative refractive index $n = -\sqrt{\mu\epsilon}$, $k^2 = n^2(\omega/c)^2$. The direction of the wave-vector \mathbf{k} with respect to the energy flow (Poynting vector) also depends on the signs of ϵ and μ :

$$\mathbf{S}(\mathbf{r}, t) = \frac{c}{4\pi}[\mathbf{E} \times \mathbf{H}] = \frac{c^2\mathbf{k}}{4\pi\omega\epsilon}H^2 = \frac{c^2\mathbf{k}}{4\pi\omega\mu}E^2. \quad (2)$$

At $\epsilon < 0$ and $\mu < 0$, vectors \mathbf{S} and \mathbf{k} become contradirected, which is in contrast with the electrodynamics of ordinary, positive index (PI) media (PIM). Such electromagnetic waves are referred to as backward or left-handed waves. Hence, magnetic response at optical frequencies, including magnetic nonlinear polarization, which does not exist in naturally occurring materials but becomes achievable in the plasmonic metamaterials, opens new avenues in electromagnetics and for its numerous revolutionary breakthrough applications.

2.0.2 Phase Matching of Counter-propagating Waves: Coupling Schemes

To explain basic principles underlying the proposal, consider nonlinear optical (NLO) coupling of ordinary and backward waves in the most simple case of continuous wave regime. Usually, negative index exist only inside a certain frequency band. The metamaterial remains ordinary, PI, outside that band. Figure 1 depict three possible options of phase matched NLO coupling of the ordinary and backward waves. Consider an

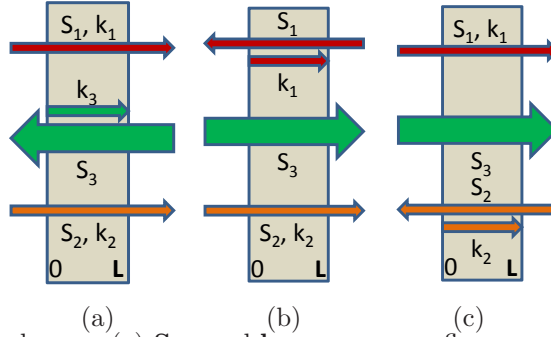


Figure 1: Proposed coupling schemes. (a) $\mathbf{S}_{1,2}$ and $\mathbf{k}_{1,2}$ are energy fluxes and wavevectors for the ordinary, positive index signal and generated idler; \mathbf{S}_3 and \mathbf{k}_3 – for the negative index control field. (b), (c) Alternative prospective schemes. (b) NLO chip amplifies signal traveling against the control beam [$n(\omega_1) < 0$] and frequency upconverts it to the contrapropagating beam. (c) NLO chip shifts frequency and reflects back the signal traveling along the control beam [$n(\omega_2) < 0$].

example depicted in panel (a). Assume that the wave at ω_1 with the wave-vector \mathbf{k}_1 directed along the z -axis is a PI ($n_1 > 0$) signal. Usually it experiences strong absorption caused by metal inclusions. The medium is supposed to possess a quadratic nonlinearity $\chi^{(2)}$ and is illuminated by the strong higher frequency control field at ω_3 , which falls into the NI domain. Due to the three-wave mixing (TWM) interaction, the control and the signal fields generate a difference-frequency idler at $\omega_2 = \omega_3 - \omega_1$, which is assumed to be a PI wave ($n_2 > 0$). The idler, in cooperation with the control field, contributes back into the wave at ω_1 through the same type of TWM interaction and thus enables optical parametric amplification (OPA) at ω_1 by converting the energy of the control fields into the signal. In order to ensure effective energy conversion the induced traveling wave of nonlinear polarization of the medium and the coupled electromagnetic wave at the same frequency must be phase matched, i.e., to meet the requirement of $\Delta\mathbf{k} = \mathbf{k}_3 - \mathbf{k}_2 - \mathbf{k}_1 = 0$. Hence, all phase velocities (wave vectors) must be co-directed. Since $n(\omega_3) < 0$, the control field is a BW, i.e., its energy flow $\mathbf{S}_3 = (c/4\pi)[\mathbf{E}_3 \times \mathbf{H}_3]$ appears directed against the z -axis. This allows to conveniently remotely interrogate the NLO converting chip and to actuate frequency up-conversion and amplification of signal directed towards the remote detector. Such signal can be, e.g., incoming far-infrared thermal radiation emitted by the object of interest, or signal that carries important spectral information about its chemical composition of the environment. The research challenge is that such unprecedented NLO coupling scheme leads to changes in the set of coupled nonlinear propagation equations and boundary conditions compared to standard ones known from the literature. This, in turn, results in dramatic changes in their solutions and in multiparameter dependencies of the operational properties of the proposed sensor.

2.0.3 Equations for Slowly-varying Amplitudes of the Coupled Fields

It is convenient to introduce the slowly-varying effective amplitudes of the waves, $a_{e,m,j}$, and nonlinear coupling parameters, $X_{e,m}$, for both, the electric (e) and magnetic (m) types of quadratic nonlinearity, $\chi_{ej}^{(2)}$, in the form:

$$a_{ej} = \sqrt{|\epsilon_j/k_j|}E_j, X_{ej} = \sqrt{|k_1k_2/\epsilon_1\epsilon_2|}2\pi\chi_{ej}^{(2)}; a_{mj} = \sqrt{|\mu_j/k_j|}H_j, X_{mj} = \sqrt{|k_1k_2/\mu_1\mu_2|}2\pi\chi_{mj}^{(2)}.$$

The quantities $|a_j|^2$ are proportional to the photon numbers in the energy fluxes. Equations for the amplitudes a_j are identical for the both types of the nonlinearities:

$$da_1/dz = iX_1a_2^*a_3 \exp(i\Delta kz) - (\alpha_1/2)a_1, da_2/dz = iX_2a_1^*a_3 \exp(i\Delta kz) - (\alpha_2/2)a_2, \quad (3)$$

$$da_3/dz = -iX_3a_1a_2 \exp(-i\Delta kz) + (\alpha_3/2)a_3. \quad (4)$$

Details can be found in [5,6]. We note the following *three fundamental differences* in Eqs. (4) as compared with their counterpart in ordinary, PI materials. First, the sign with X_3 is opposite to those with $X_{1,2}$ because $\epsilon_3 < 0$ and $\mu_3 < 0$. Second, the opposite sign appears with α_3 because the energy flow \mathbf{S}_3 is against the z -axis. Third, the boundary conditions for the control field are defined at the opposite side of the sample as compared to the signal and idler because the energy flows \mathbf{S}_3 and $\mathbf{S}_{1,2}$ are counter-directed. Indeed, this leads to *dramatic changes* in their solution and, consequently, in the propagation properties and in energy-exchange between the coupled waves in double domain PIM/NIM slab compared to those known from textbooks on nonlinear optics for their counterparts in ordinary materials.

2.0.4 Manley-Rowe Relations: Extraordinary Spatial Behavior

For loss-free ($\alpha_{1,2} = 0$), off-resonant ($X_1 = X_2 = X_3 = X = X^*$) coupling, one readily derives the following Manley-Rowe relations with the aid of equations (3) - (4):

$$d(|a_1|^2 - |a_2|^2)/dz = 0, \quad (5)$$

$$d(|a_3|^2 - |a_1|^2)/dz = 0, \quad d(|a_3|^2 - |a_2|^2)/dz = 0. \quad (6)$$

Equation (5) predicts that the difference of the numbers of photons $\hbar\omega_1$ and $\hbar\omega_2$ remains constant through the sample, which indicates their creation in pairs due to split of photons $\hbar\omega_3$. However, Eqs. (6) predict that the differences of the numbers of photons $\hbar\omega_1$ and $\hbar\omega_3$ as well as of $\hbar\omega_2$ and $\hbar\omega_3$ *also remain constant* through the sample. This looks like breaking of energy conservation law and is in seemingly striking difference with the fact that the *sum* of the corresponding photon numbers is constant in the analogous case in a PIM. Actually such unusual dependencies stem from the fact that the waves propagate in the opposite direction. Consequently, *extraordinary distributions* of these fields across the slab and the dependence of their output values on the linear and nonlinear optical properties of the given NIM and on the input intensities of the coupled fields is expected, especially when conversion efficiency become large. Particularly, conversion rate is expected to grow across the slab with a different rate than in the ordinary medium at standard coupling geometry. Equations (6) indicate unusual feedback, which provides such correlated depletion of the control field on one hand and growth of the signal and the idler on the other hand so that they difference must remain constant along the metaslab. Absorption would change such behavior which may strongly depend on the absorption dispersion and on the phase mismatch. Investigation of the indicated dependencies is important for optimization of operational properties of the proposed sensor.

3 Output Properties of the Converter and Signal Amplification

Analytical solution is not possible for the nonlinear propagation problem that underlies the concept of the sensor. Figure 2 displays the results of the numerical simulations of the model depicted in Fig 1. Here, z is the length across the slab of thickness L , $T_3(z) = |a_3(z)/a_{3L}|^2$, $T_1(z) = |a_1(z)/a_{3L}|^2$, $\eta_2(z) = |a_2(z)/a_{3L}|^2$, $g = Xa_3(L)$. Absorption indices for the coupled field are indicated, $\Delta k = 0$. Figure illustrates the case of weak input signal so that the depletion of the control field due to the conversion becomes significant only in the vicinity of $z=L$. The figure shows the possibility to achieve significant amplification of the signal travelling against the control beam and its conversion to the frequency shifted wave for the intensity of the income control field corresponding to $gL \approx 15...20$. Then the numbers of the output photons $\hbar\omega_1$ and $\hbar\omega_2$

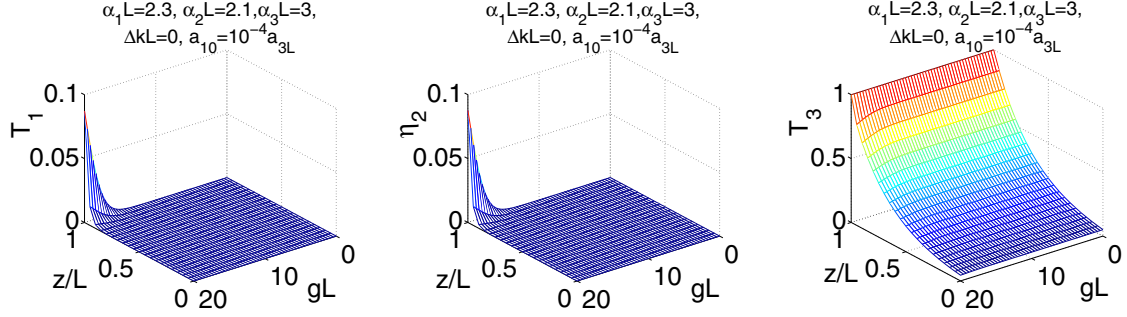


Figure 2: Distribution of the coupled fields across the metaslab and output characteristics of the amplified transmitted and generated beams as well as of the depleted control field for the case of weak input signal $a_{10} = 10^{-4}a_{3L}$.

make about 10% of that of the input contra-directed control field, which means amplification on the order of 10^7 . *Estimations* of characteristic parameters of sensor and control field based on the outlined simplified models predict that with $\chi^{(2)} \sim 10^{-5} \div 10^{-6}$ ESU ($\sim 10^3 \div 10^4$ pm/V), which is on the order of that for CdGeAs₂ crystals, the typical values of the parameter $gL \sim 1 \dots 10$ required for amplification of the signals can be achieved for a slab thickness in the *microscopic* range and for the power of the control field in the kW range with focusing on the spot of the diameter about 50 μm .

4 Conclusion

The possibility of converting strongly absorbing metamaterial slab into frequency-upconverting and amplifying nonlinear optical data processing microchip is shown and proved with numerical simulations.

5 Acknowledgments

Useful discussions with V. M. Shalaev and support of this work by the National Science Foundation under Grant No. ECCS-1028353, by the Siberian Division of the Russian Academy of Sciences under Integration Project No 5 and by the Presidium of the Russian Academy of Sciences under Grant No 27.1 are greatly acknowledged.

6 References

1. I. V. Shadrivov, A. A. Zharov, and Y. S. Kivshar, "Second-Harmonic Generation in Nonlinear Left-Handed Metamaterials," *J. Opt. Soc. Am. B*, **23**, pp. 529-534 (2006).
2. M. Scalora, G. D'Aguanno, M. Bloemer, M. Centini, N. Mattiucci, D. de Ceglia, and Yu. S. Kivshar, "Dynamics of Short Pulses and Phase Matched Second Harmonic Generation in Negative Index Materials," *Opt. Express*, **14**, pp. 4746-4756 (2006).
3. A. K. Popov and V. M. Shalaev, "Compensating losses in negative-index metamaterials by optical parametric amplification," *Opt. Lett.*, **31**, pp. 2169-2171 (2006).
4. S. O. Elyutin, A.I. Maimistov, I.R. Gabitov, "On the third harmonic generation in a medium with negative pump wave refraction," *JETP*, **111**, 157-169 (2010)].
5. A. K. Popov, "Nonlinear optics of backward waves and extraordinary features of plasmonic nonlinear-optical microdevices," *Eur. Phys. J. D* **58**, pp. 263-274 (2010).
6. A. K. Popov and T. F. George, "Computational studies of tailored negative-index metamaterials and microdevices," Chapter 13, in *Computational Studies of New Materials II: From Ultrafast Processes and Nanostructures to Optoelectronics, Energy Storage and Nanomedicine*, Edited by T. F. George, D. Jelski, R. R. Letfullin, and G. Zhang, World Scientific, Singapore, 2010.
7. S. Xiao, V. P. Drachev, A. V. Kildishev, X. Ni, U. K. Chettiar, H.-K. Yuan, and V. M. Shalaev, "Loss-free and active optical negative-index metamaterials," *Nature*, **466** (7307), 735-738 (2010).